Reliability-based structural assessment of steel truss bridges subjected to failure scenarios

López, Santiago; Barros, Brais; Buitrago, Manuel; Morales-Nápoles, Oswaldo; Adam, Jose M.; Riveiro, Belen

DOI
10.1016/j.engstruct.2025.120850

Publication date
2025

Document Version
Final published version

Published in
Engineering Structures

Citation (APA)
López, S., Barros, B., Buitrago, M., Morales-Nápoles, O., Adam, J. M., & Riveiro, B. (2025). Reliability-based structural assessment of steel truss bridges subjected to failure scenarios. *Engineering Structures*, *341*, Article 120850. https://doi.org/10.1016/j.engstruct.2025.120850

Engineering Structures 341 (2025) 120850

Contents lists available at ScienceDirect

Engineering Structures

journal homepage: www.elsevier.com/locate/engstruct

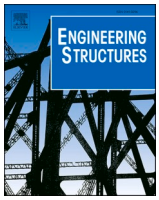

Reliability-based structural assessment of steel truss bridges subjected to failure scenarios

Santiago López [a], Brais Barros [b], Manuel Buitrago [b], Oswaldo Morales-Nápoles [c], Jose M. Adam [b,*], Belen Riveiro [a]

[a] CINTECX, Universidade de Vigo, Applied Geotechnologies Research Group, Campus Universitario de Vigo, As Lagoas, Marcosende, Vigo 36310, Spain
[b] ICITECH, Universitat Politècnica de València, Camino de Vera s/n, Valencia 46022, Spain
[c] Faculty of Civil Engineering and Geosciences, Delft University of Technology, P.O. Box 5, Delft 2600 AA, the Netherlands

ARTICLE INFO

Keywords:
Bridge
Steel truss
Reliability
Member failure
Bayesian network
Safety

ABSTRACT

Economic losses of bridge failures can mount to millions of dollars per day and spiral quickly. In particular, steel truss bridges are highly vulnerable to member failures, which, if propagated, can cause severe disruptions to the entire system. The vulnerability of these structures has been underscored in recent bridge collapses, which were initiated by the propagation of localised member failures (e.g., I-35W Mississippi Bridge). This paper proposes a methodology for the structural assessment of member failure scenarios in steel truss bridges. A quantitative index (SoD) is proposed to evaluate the consequences of member failures in all bridge elements. The methodology includes a Bayesian Network that captures the relationship between load models and structural responses. Additionally, the methodology integrates Extreme Value Analysis and computes the expected SoD for a 100-year return period. Two complementary approaches are suggested for the analysis of the member failure scenarios. The first approach focuses on the failure scenario itself, examining the post-failure effects in all bridge elements. The second approach evaluates the response of individual elements to various failure scenarios, allowing an in-depth understanding of how different member failures influence specific bridge elements. The methodology has been tested on a railway steel truss bridge in which eleven member failures were simulated. Results allowed to identify the level of significance for the scenarios, providing insights to guide SHM strategies, prioritise interventions and optimise maintenance efforts. This work aims to simplify engineering efforts and support bridge management entities in their crucial fight to improve the bridge's structural safety.

1. Introduction

Societies are confronting unprecedented extreme events that surpass existing adaptation efforts [1]. Civil infrastructures are increasingly exposed to aggressive environmental conditions, rising traffic loads, and maintenance deficiencies, exacerbating structural deterioration over time [2]. These destabilizing factors have considerably magnified the socioeconomic impacts on transportation networks [3]. Steel truss bridges, in particular, are increasingly vulnerable to member failures that, under adverse conditions, may initiate a cascade of structural damages across the entire bridge system, leading to progressive collapse [4–6]. Bridge collapses often result in devastating consequences, including fatalities, service disruptions, and significant economic and environmental losses [7–9]. Due to the importance of such a phenomenon and its relevance to our society, progressive collapse has become one of the most active research areas in structural engineering [10–12]. This highlights the urgent need to assess member failure scenarios in steel truss bridges. Understanding how these localised failures impact the overall stability of such structures is essential to prevent progressive collapse.

Over the last decade, several efforts have been made to assess member failure scenarios in steel truss bridges [13–26]. These studies have been conducted broadly through experimental approaches, numerical modelling, or a combination of both. Among the most relevant experimental studies, Buitrago et al. [13] tested a 21 m full-scale steel truss bridge with an extensive monitoring system subjected to member failure. Their work established practical structural health monitoring recommendations to identify early failures. Similarly, Brunell et al. [14] tested a laboratory-scale steel truss bridge under 16 damage scenarios. The study aimed to propose a global safety index as an indicator to

* Corresponding author.
E-mail address: joadmar@upv.es (J.M. Adam).

https://doi.org/10.1016/j.engstruct.2025.120850
Received 10 March 2025; Received in revised form 30 May 2025; Accepted 20 June 2025
Available online 26 June 2025

detect the presence of local damage. Zhao et al. [15] designed a member-breaking device to remove a member in planar trusses suddenly, and a collapse-resistant analysis for different element-removal cases was performed. On the other hand, among the most relevant studies in which numerical modelling has been implemented to assess member failures in steel truss bridges, Porcu et al. conducted a robustness-based assessment in a steel truss bridge to prevent progressive collapse [16], eight failure scenarios were considered in the study, and their role on the progressive collapse was analysed. Caredda et al. [17] analyse different member failure scenarios in a validated FEM to assess the steel truss bridge capacity to activate Alternative Load Paths (ALPs) efficiently. Chen et al. [18] performed an ALP-based methodology, which includes two quantitative metrics to analyse the redundancy of steel truss bridges subjected to member failure scenarios. Praxedes et al. [19] developed a probabilistic-based robustness index for the analysis of the progressive collapse of a bridge subjected to an unexpected element failure. Li et al. [20] developed a framework that considers the dynamic effect of sudden member loss to identify critical members in steel truss bridges. Lastly, Connor et al. [21] developed a model-based standardized methodology to identify fracture-critical members in steel truss bridges; these findings were published in official guide specifications [27,28].

As seen, most of the research conducted to assess scenarios of member failures in steel truss bridges has been concentrated on encompassing strategies to determine the ability of the bridge to withstand when a local failure occurs; this approach has been demonstrated to be essential to develop the knowledge on bridge redundancy and structural robustness [29–31]. Nevertheless, a reliable quantitative assessment that evaluates the consequences at the element level remains undeniably crucial to understanding the impact of localised failures in the entire structure. Beyond that, it is equally essential to determine whether failure-induced demand alterations remain localised or propagate throughout the truss system. Such insights would allow for prioritising bridge elements, serve as a decision-making tool to optimise SHM systems, and directly enhance the safety and reliability of steel truss bridges.

Bridges deteriorate over time due to exposure to aggressive environments and increasing traffic loads [32]. This degradation leads to a progressive reduction in structural reliability, which may eventually fall below acceptable safety levels [33]. Uncertainties in bridge assessments arise in multiple aspects, including material mechanical properties, operational and environmental conditions, and applied loads [34–36]. In response, reliability-based approaches have emerged to quantify these uncertainties and enhance the structural assessments [31]. Traditionally, structural reliability has been evaluated using conventional methods [37–39]. However, Bayesian Networks (BNs) have given rise to a significant research trend, having emerged as a promising alternative for conducting reliability assessments [40–42]. It has been shown that BNs offer substantial advantages over traditional frameworks due to their ability to characterise and analyse uncertainty effectively [43]. The applications of BNs in bridge engineering have been extended to many fields involving bridge safety [44–49], risk analysis [50–53], damage detection [54–57] and FE advance modelling and updating [58–61]. One of the most important applications of BNs for reliability applications involves the probabilistic modelling of traffic loads [62–68]. This approach has proven to be effective in enhancing the robustness of structural assessments [69]. In this regard, Morales-Napoles et al. [62] developed a large-scale BN for traffic load modelling using Weigh-In-Motion (WIM) data. Mendoza-Lugo et al. [63] proposed a BN to generate synthetic heavy loads and estimate the criticality of the national bridge network of Mexico. Kim et al. [64] developed a Bayesian updating methodology for the probabilistic modelling of bridge traffic loads using in-service SHM data. Lastly, Yu et al. [65] implemented a BN for the condition assessment of bridges; the BN was designed to predict the extreme load effects. While BNs have been widely employed in bridge reliability assessments, a significant gap remains in their integration with FEM-based methodologies. Existing studies have primarily focused on traffic load modelling or direct condition assessments but have not leveraged BNs to establish a probabilistic link between load conditions and structural response within a reliability-based framework.

The analysis of demand effects (e.g. displacements), particularly the Extreme Values of the Demand Effects (EVDE) is also essential to assess the reliability of bridges [70]. Typically, these methods consider the simulation through a FEM-based approach [71], applying recorded data of real traffic (e.g. WIM stations) [72]. However, significant gaps are limiting the accuracy and applicability of this approach [73]. On the one hand, the estimation of EVDE relies on extreme demands that, are rarely observed on real recorded data. On the other hand, recorded traffic data, in turn, is commonly restricted to a short time period [72]. In response, various probabilistic methods have been developed to estimate EVDE on structures [74–78]. The estimation of EVDE in bridges is an ongoing focus of research within bridge engineering [79–82]. Wang et al. [79] performed an analysis in a cable-stayed long-span bridge to assess the extreme load effects based on vehicle distribution and its location through the bridge; the study was further extended for vehicle-congested conditions [80]. Rahman et al. [81] performed component-level and system-level fragility analyses for the resilience of coastal bridges exposed to extreme waves. Dai et al. [82] simulated the 100-year response of bridges of various spans to develop an algorithm able to fit data from WIM systems and predict extreme values responses. Despite its extensive applications, existing approaches of EVDE have primarily focused on global load effects, without considering the impact of member failures under extreme demand conditions. This study bridges this gap by integrating EVDE estimation in bridges subjected to localised failure scenarios.

This study introduces a novel methodology for the structural assessment of steel truss bridges subjected to localised member failures. While previous research has focused on robustness evaluation or structural collapse prevention, this work advances the field by implementing a dual-analysis perspective to understand how failures affect all bridge elements and how each element responds to multiple failure scenarios. The methodology integrates the quantification and propagation of uncertainties to calibrate a finite element model (UFEM). A Gaussian Copula-based Bayesian Network (GCBN) is employed to model the operational loads on the structure, providing a probabilistic representation of train axle loads which accounts for possible variations in train weights. These probabilistic load scenarios are propagated through the UFEM to compute the State-of-Demand (SoD) index for all structural elements, enabling a quantitative assessment of the demand state of the structural elements in the entire bridge. Finally, Extreme Value Analysis (EVA) is applied to estimate SoD values for long-term return periods, supporting the identification of critical elements and prioritisation of maintenance actions. The main novelty of this study lies in the development and implementation, in a real-world case study, of a unified reliability-based methodology that comprehensively quantifies the effects of member failure scenarios in steel truss bridges by integrating uncertainty quantification and propagation, probabilistic load modelling, and the application of extreme value theory.

The objective of this study is to propose a methodology for the structural assessment of member failure scenarios in steel truss bridges, addressing key gaps in existing methodologies. A quantitative index (SoD) is proposed to evaluate the consequences of member failures. The State-of-Demand index (SoD) quantifies the relationship between demand and capacity on each bridge element when the bridge is subjected to member failures. Additionally, a Gaussian Copula-based Bayesian Network (GCBN) is developed to model the probabilistic relationship between loading conditions and structural response (SoD). This allows for the generation of critical load conditions while incorporating uncertainties inherent to bridge loading. The proposed methodology integrates two complementary analysis approaches. First, the structure-level analysis, which focuses on the failure scenario itself, examining

the post-failure effects in all bridge elements. Second, the element-level analysis, which evaluates the response of different bridge elements when the bridge is subjected to several member failure scenarios. The methodology is validated in a real railway steel truss bridge. The methodology provides valuable insights to guide SHM strategies, prioritising interventions, optimise maintenance efforts, and enhance risk assessment methodologies.

After this introduction, Section 2 presents the proposed methodology. This Section details the Updated Finite Element Model (UFEM) and introduces the SoD which is used as a key performance metric. Additionally, the implementation of a GCBN for generating critical load conditions is described, along with the application of EVA to estimate SoD extremes over long-term return periods. Section 3 applies the methodology to a real steel truss bridge. Two complementary analyses are implemented, the element-level and the structure-level analyses. Finally, Section 4 highlights the findings of this research with the main conclusions drawn from the work.

2. The methodology

This section presents the methodology for evaluating the impact of different member failure scenarios in steel truss bridges at both structure and element levels. The proposed methodology ultimately integrates numerical modelling, structural performance metrics, and statistical tools to propose an approach for assessing failure scenarios in steel truss bridges. The methodology is conducted using an updated finite element model (UFEM), in which member failure scenarios are numerically simulated. For each bridge element (e.g. an upper chord), the State-of-Demand index (SoD) is computed as a core metric for quantifying the differences between structural demand and capacity (see 2.2). In this regard, Extreme Value Analysis (EVA) is applied to estimate the SoD extremes for various return periods (e.g., SoD for a 100-year return period) (see 2.3). Recognizing the critical influence of the load characterisation, the methodology includes a Gaussian Copula-based Bayesian Network (GCBN) to generate realistic loading conditions (see 2.1). Two analysis approaches are employed to assess the bridge subjected to member failure scenarios; both are described in the last part of this Section (see 2.4). The flowchart of the methodology is presented in Fig. 1, highlighting the stages of the methodology. The stages are explained in detail in the following subsections. The reader is referred to Section 3 for the practical application of these concepts on a real steel truss bridge.

2.1. The state-of-demand index (SoD) of individual elements

The methodology considers a quantitative index to evaluate the elements demand state in relation to reference values related to its capacity. Several indexes have been developed in the literature in this regard [22–24]. In this study, the State-of-Demand index (SoD) is adopted as core numerical metric. The SoD is computed through the Updated Finite Element Model (UFEM). The SoD is formulated as a set of ratios reflecting the state of each bridge element based on two criteria: (i) proximity to steel yielding (and (ii) susceptibility to local instabilities (). Thus, the SoD is selected as the higher of the Demand Capacity Ratio (DCR) of axial forces and stresses, as follows:

$$SoD_{element,n} = \max(DCR_{AF} \quad , DCR_S) \tag{1}$$

Where the Demand Capacity Ratio of axial forces () is computed as follows:

$$DCR_{AF} = \frac{P_{num}}{P_{cr}} \tag{2}$$

P_{num} is the Numerical Axial-Force computed during each iteration, while P_{cr} is the critical buckling load according to the Euler's formulation. P_{cr} is calculated as described in Eq. (3), where E represents the modulus of elasticity of the steel, I is the moment of inertia of the element under analysis, k is the element effective length factor and L denotes the element length.

$$P_{cr} = \frac{\pi^2 EI}{(kL)^2} \tag{3}$$

The Demand Capacity Ratio of stresses () is computed as described in

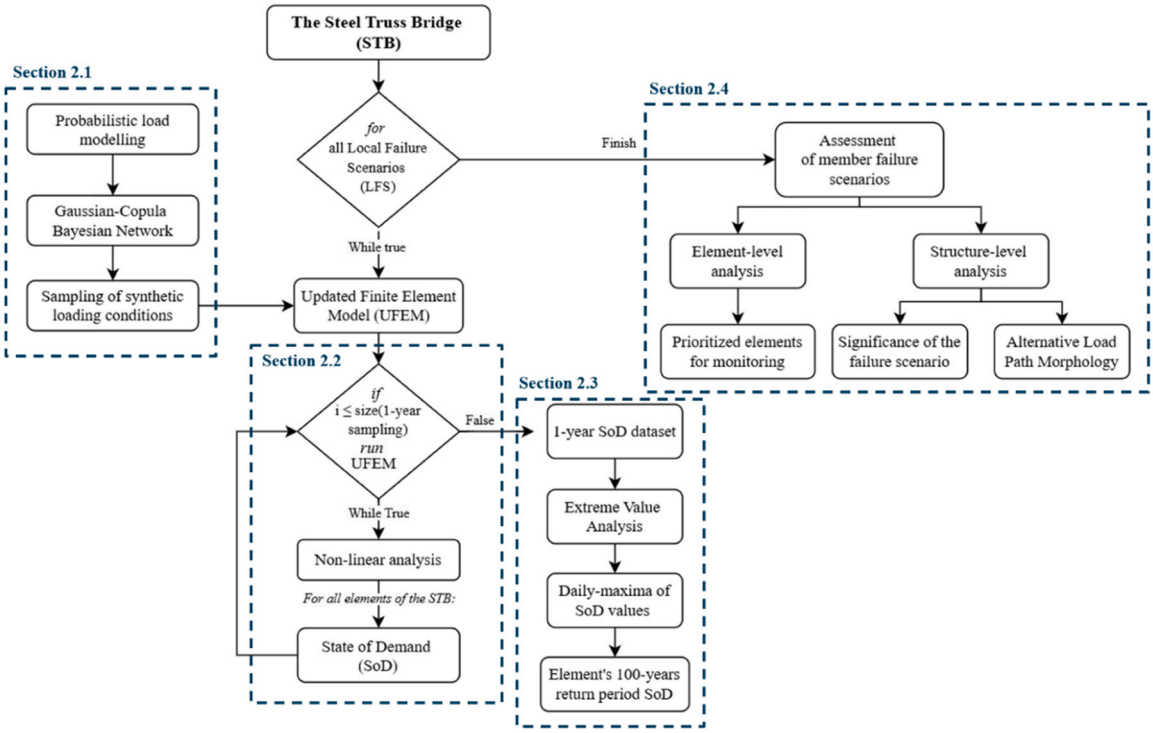

Fig. 1. Flowchart of the methodology.

Eq. (4) where σ_{num} is the Numerical Von Mises Stress and f_y is the steel yield strength.

$$DCR_S = \frac{\sigma_{num}}{f_y} \tag{4}$$

In this study, SoD is implemented to assess the structural response of all bridge elements when a member failure occurs (e.g. the failure of a lower chord). The SoD is computed individually for each structural element (e.g., an upper chord) as a result to propagate through the UFEM the extreme loading conditions generated by the GCBN (refer to Section 2.2). Thus, the SoD is recalculated in every realisation under extreme loading conditions. As depicted in Eqs. (2) and (4), the capacity-related reference values to compute and are defined based on the yielding of the cross-section (f_y) and Euler's critical load (P_{cr}), which are assigned from the calibrated model and remain constant. Therefore, the SoD reflects how close each element is to its structural capacity under extreme loading conditions. This makes the SoD a reliable indicator for the element-based structural assessment of steel truss bridges subjected to failure scenarios.

2.2. Probabilistic load characterisation

The probabilistic load characterisation is a fundamental component of the methodology presented in this study. This section outlines the essential considerations for accurately characterise the loads and integrating them into the methodology. Initially, the section establishes the key criteria for selecting an appropriate load model and determining its critical position on the bridge. Subsequently, a four-stage procedure to create a Gaussian Copula-based Bayesian Network (GCBN) to integrate the load model and the structural response (SoD) is presented.

2.2.1. Load model and critical load position on the bridge

The load model and its configurations depend on the specific conditions of the bridge. These conditions include its usage (e.g., railway bridge) and the type of traffic it supports (e.g., passenger, freight). Ideally, the load model should be adopted based on real traffic data (e.g. a WIM system) to reflect the operational conditions of the structure and how the load is distributed along the convoys. However, this approach is not always feasible; alternatively, the load model may be selected based on official standards [83]. Once the load model is determined, identifying its critical position on the bridge is essential. This process typically involves simulating multiple loading scenarios in different positions along the structure to analyse the load position that produces the most critical effects on the bridge. Undoubtedly, the critical load position is not unique, this is even more relevant when dealing with failure scenarios located at different positions of the structure. Thus, the critical load position is considered as the first to occur of: (i) The load position that induces the highest overall mean of SoD across all bridge elements (see 2.2), or, (ii) the load position which generates the earlies failure to the structure (no-convergence criteria). However, any method [84,85] that systematically seeks the most adverse conditions to the structure is also applicable.

2.2.2. Gaussian Copula-based Bayesian Network

The methodology incorporates a Gaussian Copula-based Bayesian Network (GCBN) to integrate the load model and the structural response, represented by the SoD. The primary purpose of the GCBN is to generate samples that reflect critical (but realistic) loading conditions for the bridge. To this, the variables of the load model (e.g., train axle loads) and the structural response (SoD) are represented as nodes in the GCBN, with their dependencies captured through arcs defined by correlation coefficients. These coefficients characterise the strength and nature of the relationships between nodes, enabling the network to encode complex joint probability distributions efficiently. This capability allows for inference within the GCBN (e.g., conditioning on the SoD) to generate synthetic samples of load variables that reflect critical loading conditions.

The GCBN is structured as a Directed Acyclic Graph (DAG), where each node represents a continuous random variable, and the edges are assigned (conditional) bivariate copulas to capture conditional dependencies between the random variables. The graph in itself contains conditional independence statements usual in Bayesian Networks. Fig. 6 (b) illustrates the configuration used for the case study, where load variables (PL1 to PL5) act as parent nodes, and the structural response (mSoD) is introduced as a child node in the GCBN.

The dependence structure in the GCBN is built using a Gaussian copula, which enables the construction of a joint distribution with given marginal distributions and a correlation matrix. For two uniform random variables $(u, v) \in [0,1]^2$, the Gaussian copula is defined as:

$$C_\rho(u,v) = \Phi_\rho\left(\Phi^{-1}(u), \Phi^{-1}(v)\right) \tag{5}$$

Where Φ^{-1} denotes the inverse of the univariate standard normal cumulative distribution function and Φ_ρ is the bivariate standard normal cumulative distribution function with linear correlation coefficient ρ. This construction decouples marginal distributions from their dependence structure.

The joint probability distribution across all nodes is factorised using the DAG structure as:

$$f(x_1, \ldots, x_n) = \prod_{i=1}^{n} f(x_i | pa(x_i)) \tag{6}$$

Where each conditional density $f(x_i|pa(x_i))$ is determined by the marginal $F_i(x_i)$ and the copula-based dependency between the variable and its parents. Conditional rank correlations are used to quantify the dependencies. For a node X_i with parent nodes $pa_1(X_i), \ldots, pa_m(X_i)$, the rank correlation is assigned as:

$$r\left(X_i, pa_j(X_i) \,|pa_1(X_i), \ldots, pa_{j-1}(X_i)\right) \quad j = 2, \ldots, m \tag{7}$$

$$r\left(X_i, pa_j(X_i)\right); j = 1 \tag{8}$$

These rank correlations are mapped to Pearson correlation coefficients in the Gaussian copula using:

$$\rho = \sin\left(\frac{\pi}{6} r\right) \tag{9}$$

Since partial correlations are equal to conditional correlations in the multivariate Gaussian case. Then, the correlation matrix is assembled using the usual recursive formula:

$$\rho_{1,2;3,\ldots,n} = \frac{\rho_{1,2;4,\ldots,n} - \rho_{1,3;4,\ldots,n}\rho_{2,3;4,\ldots,n}}{\left(\left(1 - \rho^2_{1,3;4,\ldots,n}\right)\left(1 - \rho^2_{2,3;4,\ldots,n}\right)\right)^{1/2}} \tag{10}$$

The assignment described until now. Ensures a valid correlation matrix. While the main assumption of the model is that the Gaussian copula adequately represents the data. One of the key advantages of this formulation is the ability to perform inference. Given an observed or target value y of a variable Y, the GCBN enables conditional sampling of the remaining variables X. Conditionalizing in GCBN is efficient since the conditionalization is done in the multivariate standard normal transform of the variables. This allows for the generation of load scenarios that are statistically consistent with a desired structural response (e.g., high mSoD).

This section describes the process for developing the proposed GCBN. Although the process intends to be standard, it is crucial to note that for the practical application a self-judgement must be exercised based on the purpose of the GCBN, which is to reduce uncertainties in the load model. The logical process for creating the GCBN is outlined through a systematic four-stage procedure. For the practical application of a GCBN to characterise the loading conditions in a real structure the reader is referred to Section 3.

1. The first stage involves constructing an Initial Gaussian Copula-based Bayesian Network (IGCBN). This stage involves the creation of an initial directed acyclic graph (DAG) and the selection of the probabilistic parameters of the nodes. In the initial DAG, the nodes should correspond to the load model variables (e.g. train axle weights). It is essential to select the node parameters (mean and standard deviation) based on engineering judgment of the real conditions. If the assessment includes traffic observations (e.g., with a WIM system), the parameters should be derived directly from observations; otherwise, the parameters should be assigned based on standards [83]. Ultimately, the IGCBN is constructed to represent variability in loading conditions.
2. The second stage focuses on evaluating the influence of probabilistic dependencies of the IGCBN in the global structural response. This involves performing a sensitivity analysis in the IGCBN to analyse how its probabilistic dependencies affect the SoD in all bridge elements. To achieve this, the IGCBN is used to sample loading with varying correlation coefficients (CCs) (e.g. 0.8, 0.9, 0.95). The sensitivity analysis is performed through the UFEM, where the mean value of the SoD (mSoD) is analysed for all bridge elements. mSoD quantifies the entire bridge demand state, higher mSoD's indicate that, on average, the bridge elements experience high demand ratios in relation to their capacities.
3. The third stage aims to evaluate the results of stage 2 to generate a dataset that will be used to create a final GCBN. As the GCPN aims to generate critical loading condition for the bridge, this stage focuses on selecting the samples (loads) that resulted in the highest structural demands (mSoD) from the simulations performed with different CCs (stage 2). A package-based approach is considered, where a subset of the samples (e.g., a decile) with the highest mSoD are selected from each group of simulations (corresponding to different CCs). Each package includes both the samples (loads) and the responses (mSoD's) for all CC groups of simulations. The generated packages are then combined in a final dataset, which includes the highest-demand scenarios across all CC groups.
4. The final stage involves updating the IGCBN by incorporating the effects of the loads on the bridge (final dataset). This is achieved by adding an additional node to the DAG, representing the global structural response (mSoD). The mSoD node will then modify the network dependencies, becoming the parent of the nodes representing the load system variables. The parameters of the updated GCBN are calculated by fitting to theoretical distributions (e.g., Gaussian, Gumbel, Weibull, etc…) the variables of the final dataset performed in Stage 3. This process results in a GCBN that integrates the uncertainties in the loading conditions and their structural effects. The final GCBN can infer the load conditions that would lead to a specific demand state for a defined time period (e.g. 1 year of loading conditions for 20 trains passing per day).

The GCBN developed in this work stands out as a versatile and powerful tool for structural engineering. Although the GCBN is used in this study to generate critical (but realistic) loading, its capability goes far beyond that [86]. In general, the GCBN can be used to infer any variable within the network through conditionalization, making it invaluable for reliability studies and allowing the analysis of complex interactions between loading conditions and structural responses. Additionally, the GCBN benefits practitioners by providing a practical tool to determine the structure demand state through its loading condition. This dual capability highlights the GCBN as an essential resource for both advanced reliability-based analyses and practical structural evaluations, demonstrating its adaptability to a wide range of structural engineering applications.

2.3. Extreme SoD effects

The analysis of the demand effects (e.g. displacements), particularly the Extreme Values of the Demand Effects (EVDE), is essential to assess the reliability of bridges [66]. This discipline, known as Extreme Value Analysis (EVA) [87] considers the application of statistical techniques to fit a distribution of demands (e.g. displacements) to the tail of its cumulative distribution function (CDF) [70]. The most common methods employed to estimate EVDE are the Peaks-Over-Threshold (POT) method [74] and the Block Maximum (BM) method [75]. POT assesses the extent to which peaks exceed a specified threshold [74], fitting these peaks to a probability distribution such as the Generalized Pareto distribution (GP) [76]. BM, by contrast, considers only the maximum demand effects in a predefined time block [75], which is advantageous for calculating lifetime maximum probabilities of exceedance. Other alternative methods, such as the Box–Cox method [77] and Rice formula [78], are also employed.

As discussed, the GCBN (see 2.2) can generate loading conditions for a defined time period (e.g. 1 year of loading conditions for 20 trains passing per day). These loading conditions are subsequently used as input in the UFEM to compute the SoD for all bridge elements. Thus, EVA is employed in this work to assess, for all bridge elements, the extreme structural responses (SoD) when the bridge is subjected to member failure scenarios.

This study adopts BM fitting to a Generalized Extreme Value distribution (GEV), given that this approach considers only the largest event in each time block (e.g. a one-day block), and its usefulness lies in its ability to effectively capture daily variations, offering a versatile approach adaptable to a variety of scenarios [75]. This capability makes it particularly advantageous for EVA, establishing it as fundamental in recent studies [79–82]. In this study, BM is fitted to the GEV distribution as described in Eq. (1). Where μ is the location parameter, σ is the scale parameter, and ξ is the shape parameter. There are three types of extreme value distributions characterised by the parameter ξ. When the parameter ξ equals 0, the distribution is a Gumbel distribution; when ξ is greater than 0, it is a Fréchet; and when ξ is less than 0, it is a Weibull distribution.

$$F(x;\mu,\sigma,\xi)=\begin{cases}\exp\left(-\left(1+\xi\left(\frac{x-\mu}{\sigma}\right)^{-\frac{1}{\xi}}\right)\right), \&\xi\neq 0\\ \exp\left(-\exp\left(-\frac{x-\mu}{\sigma}\right)\right), \&\xi=0\end{cases} \tag{11}$$

In the context of this work, the methodological process starts with grouping the SoD data in one-day blocks, with the maximum value recorded in each block (daily maxima). The maximum likelihood estimation (MLE) method determines the parameters that best fit the daily maxima data to the GEV. Once the GEV is characterised, its empirical cumulative distribution function (ECDF) is calculated, which is then used to determine the expected SoD value across various return periods (T). Return periods provide a probabilistic approach to quantify the occurrence of SoD extremes, offering insight into the frequency at which a SoD might be expected over a given timeframe [88]. Return periods define the expected time (in years) between exceedances of a specific SoD (e.g. an event with a 1 % annual probability of exceedance corresponds to a return period of 100 years, T_{100}). Ultimately, the methodology focuses on the SoD associated with a 100-year return period ($SoDT_{100}$) which is computed for all bridge elements while it is subjected to all damage scenarios. The final output of this methodology is an $n \times m$ matrix, where n represents the $SoDT_{100}$ for all bridge elements at m member failure scenarios considered. For the practical application of EVA to assess the SoD extremes in a real structure, the reader is referred to Section 3.

2.4. Assessment of member failure scenarios

This section defines the methodology to analyse the SoD associated with a 100-year return period ($SoDT_{100}$) of all bridge elements for the

bridge subjected to member failure scenarios. The analysis is performed by computing the absolute difference of the $SoDT_{100}$ for a given bridge element (e.g. the $SoDT_{100}$ of an upper chord when a lower chord failure occurs) with its undamaged state (the $SoDT_{100}$ of the same upper chord for the bridge on its undamaged state). This metric, here called $\Delta SoDT_{100}$ (see Eq. (2)), is computed for all bridge elements and failure scenarios considered.

$$\Delta SoDT_{100} = \left| SoDT_{100\ \ scenario} - \ \ SoDT_{100\ \ undamaged} \right| \tag{12}$$

Two complementary approaches are employed in the analysis. The first approach (structure-level) focuses on the failure scenario itself, examining its effect on the $\Delta SoDT_{100}$ values of all bridge elements post-failure. The second approach (element-level) evaluates the response of individual elements to various failures, allowing an in-depth understanding of how these scenarios influence specific bridge elements. The following lines describe both approaches in detail. The reader is referred to Section 3.3 for the practical application and analysis of both analysis approaches in a real steel truss bridge.

2.4.1. Structure-level analysis

The structure-level analysis focusses into analyse how a specific member failure scenario (e.g. the failure of an upper chord) affects the $\Delta SoDT_{100}$ of all bridge elements (e.g. Diagonals, verticals, lower chords, etc.). This approach aims to analyse the scenario significance. A member failure scenario is deemed significant if it induces in any bridge element increases of the State-of-demand ($\Delta SoDT_{100}$). As an example, the following categorical scale is proposed to classify each scenario by its level of significance:

- $0 \leq \Delta SoDT_{100} < 5$, low significance scenario.
- $5 \leq \Delta SoDT_{100} < 25$, low-medium significance scenario.
- $25 \leq \Delta SoDT_{100} < 60$, medium significance scenario.
- $60 \leq \Delta SoDT_{100} < 100$, medium-high significance scenario.
- $\Delta SoDT_{100} \geq 100$, high significance scenario.

2.4.2. Element-level analysis

The element-level analysis centres to analyse the $\Delta SoDT_{100}$ of a specific bridge element (e.g. a midspan diagonal) or groups (e.g. diagonals) for all member failure scenarios. Element-level analysis ultimately identifies elements that should be prioritised in the structural health monitoring (SHM) and maintenance systems. Although the prioritisation hierarchy should encompass an engineering judgment of the undamaged state of the element, an element in which the $\max(SoDT_{100\ \ for\ all\ scenarios})$ is considerably higher in relation with its undamaged state ($SoDT_{100\ \ undamaged}$) should be prioritised.

3. Application to a real steel truss bridge

The methodology described in Section 2 has been tested in a railway steel truss bridge. This bridge was selected as a case study due to its characteristics as an old-riveted steel truss structure with available monitoring data. Additionally, it has been previously analysed, emerging as an engaging alternative for selecting relevant member failure scenarios. At the outset, this section describes the bridge and the procedure adopted to achieve a calibrated Updated Finite Element Model (UFEM). In the first stage, the load model is described. The procedure to generate a Gaussian Copula-based Bayesian Network (GCBN) to generate 1-year of critical loading conditions is addressed. The discussion continues with selecting member failure scenarios based on historical precedents and an in-service structural assessment. Subsequently, for each member failure scenario, the State-of-Demand (SoD) index is computed for all bridge elements. Extreme Value Analysis (EVA) is then employed to compute the 100-year return period of the SoD. Finally, the last part of this section presents and discusses the results of the methodology. The discussion is addressed by analysing two complementary approaches. While the first approach evaluates the impact of each member failure scenario on the bridge elements, the second approach examines how different bridge elements respond to all member failure scenarios.

3.1. Description of the bridge

The bridge consists of a three-isostatic-span steel truss bridge located in Galicia, Spain. The bridge, constructed in 1910 [89], has a span length of 40 m for the side spans and 70 m for the central span. This study only considers one side span (40 m length, 7 m width, and a maximum height of 8 m). The arch (upper chords) has a parabolic shape, and both sides are connected by five transversal beams. These upper chords are vertically linked to the bottom chord through fourteen verticals and four piers. The deck is formed by nine transversal beams and thirty-two lower bracings, equally divided into eight panels of four members each. The lower bracings run directly beneath the projection of the traffic lanes (interior longitudinal beams), and the loads can be applied directly onto these elements. The bridge presents simple hinged supports on one side and roller-hinged supports on the other. During the construction, all members were built up using steel plates and L-type profiles joined by rivets. Fig. 2 shows a downstream view of the bridge.

An initial finite element model (IFEM) of the bridge was developed using data gathered from an experimental campaign. The campaign involved a detailed visual inspection that identified widespread corrosion, thickness losses, and other damage in various structural components. A Terrestrial Laser Scanning (TLS) survey was conducted to produce a high-resolution point cloud model of the structure. An Ambient Vibration Testing (AVT) complemented the campaign with a multi-setup deployment of seismic accelerometers capturing the dynamic behaviour of the bridge. The collected data informed the as-built geometric modelling. The initial FEM was modelled using DIANA FEA [79] and was connected via MATLAB [80]. The model updating was carried out through a genetic algorithm to minimize discrepancies between numerical and experimental results. The updated model achieved a mean frequency error of 3.24 % and a Modal Assurance Criterion (MAC) average of 0.947, demonstrating high agreement between experimental and numerical behaviour. The study presented here relies on a nonlinear analysis accounted for both physical and geometrical nonlinearities performed in the Updated Finite Element Model (UFEM). The UFEM is shown in Fig. 3.

The load characterisation of the bridge was conducted as described in Section 2.2. The bridge is located in an industrial area frequently used by passenger and freight trains. Thus, the Type 5 locomotive-hauled freight train from the Eurocode was selected [90]. The UFEM was configured to compute the analysis of the critical loading position, where the load was applied acting on nodes on the interior longitudinal beams. Several analyses were simulated varying the point load positions

Fig. 2. The steel truss bridge.

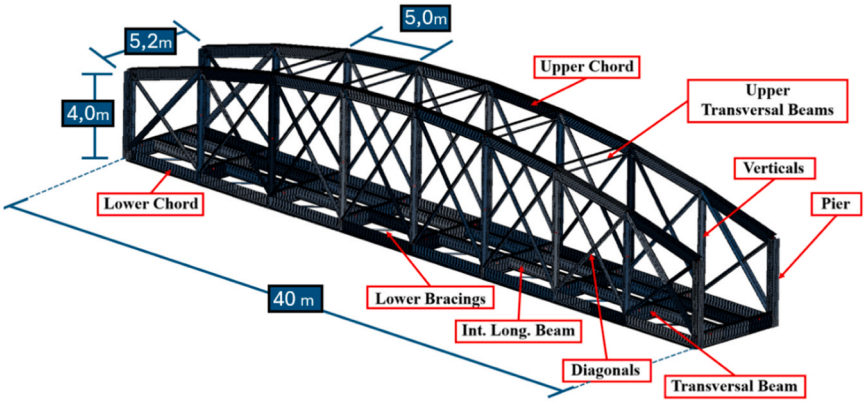

Fig. 3. 3D-View of the Updated Finite Element Model (UFEM).

at different locations along the bridge span. The criteria for identifying a load position as critical were those defined in Section 2.2. Fig. 4 presents the adopted load model, while Fig. 5 highlights the critical load position after performing the abovementioned analysis on the structure.

3.2. Failure scenario definition

The characterisation of the member failure scenarios is addressed in this section. The approach to generate critical loading conditions is presented. Then, the selection of relevant member failures is discussed. Specifically, this section aims to create a GCBN that integrates the load model with the SoD. In addition, the reasoning behind selecting candidate elements to simulate their failure in the UFEM is discussed. This section ultimately illustrates the practical application of the methodology described in Section 2 adapted to the specific characteristics of the case study.

3.2.1. Generation of synthetic heavy trains

Building upon the updated finite element model (UFEM) described in Section 3.1, the four-stage procedure outlined in Section 2.2.2 was followed to create a GCBN to generate loading samples represented critical conditions for the bridge (synthetic heavy trains). The GBPN has been implemented in BANSHEE, an open-access scriptable code developed as a toolbox in MATLAB [91] and Python [92,93]. In this work, the MATLAB version of BANSHEE was employed.

The process started with the construction of the initial DAG. Each group of six-point loads (PL1, PL2, …, PL6) in the load model was defined as one node in the DAG, as illustrated in Fig. 6a. The mean SoD was selected as the parent node (see 2.2.2). The mean value for the load nodes (PL1 to PL5) was derived directly from the load model (see Fig. 4). Since 80 % of the total load was attributed to the locomotive's dead weight, the standard deviation of the load nodes was calculated based on two scenarios: fully loaded wagons and empty wagons (where empty wagons will weigh 20 % less than fully loaded ones). The probabilistic dependencies among load variables and mSoD were incorporated as correlation coefficients (CCs) between DAG arcs. Stage 2 in 2.2.2 was implemented to assess the influence of probabilistic dependencies of the IGCBN in the global structural response (mSoD). CC values of 0.6, 0.7, 0.8, 0.9, and 0.95 were considered. For each simulation group with its corresponding CC (e.g. simulation group of CC = 0.6), 1000 synthetic train samples were generated, and the mSoD was computed using the UFEM. As described in stage 3 in 2.2.2, a package-based approach was employed to identify the fifty highest-demand scenarios for each simulation group. This stage finally compiled a dataset containing the highest demand loading conditions (PL1 to PL5) alongside their corresponding mSoD responses.

The resulting dataset was fitted to theoretical probabilistic distributions; the results are illustrated in Fig. 7, where each node of the IGCBN is presented with its corresponding theoretical distribution. As seen in the figure, the data for the five load nodes (PL1 through PL5) were fitted to normal distributions, with mean values significantly higher than those suggested by regulatory standards (see Fig. 7). In contrast, the mSoD node was fitted to a Generalized Extreme Value (GEV) distribution, characterised by its tail dependency. The specific parameters of the GEV distribution (k, μ, and σ) are also presented in Fig. 7. These fitted parameters provide the probabilistic basis for the characterisation of the final GCBN, which integrates the mSoD as a parent node to the load nodes (PL1 through PL5). The final GCBN establishes a hierarchical structure that captures the dependencies between the structural response and the load variables. This integration models the global structural response of the bridge while maintaining the variability and interactions between the load nodes. The correlation matrix of the final GCBN is presented in Fig. 8.

The GCBN is used to generate synthetic heavy trains, which involves sampling loading conditions (PL1 to PL5). This process relies on conditional inference [94], a mathematical approach where the

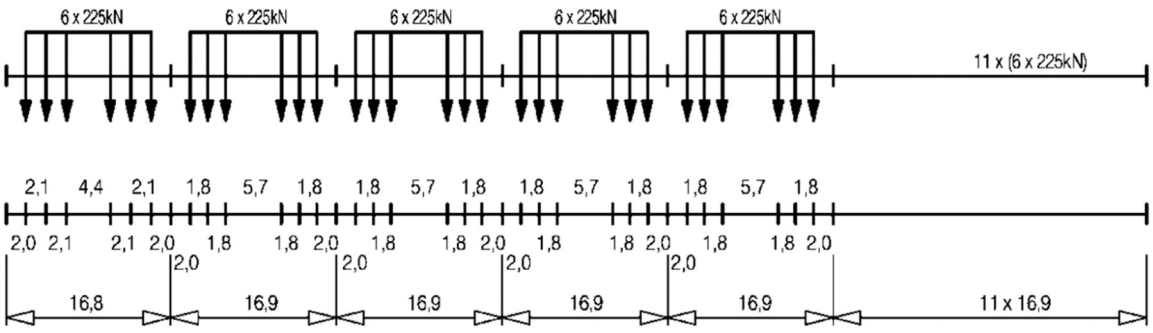

Fig. 4. Load model adopted. From [90].

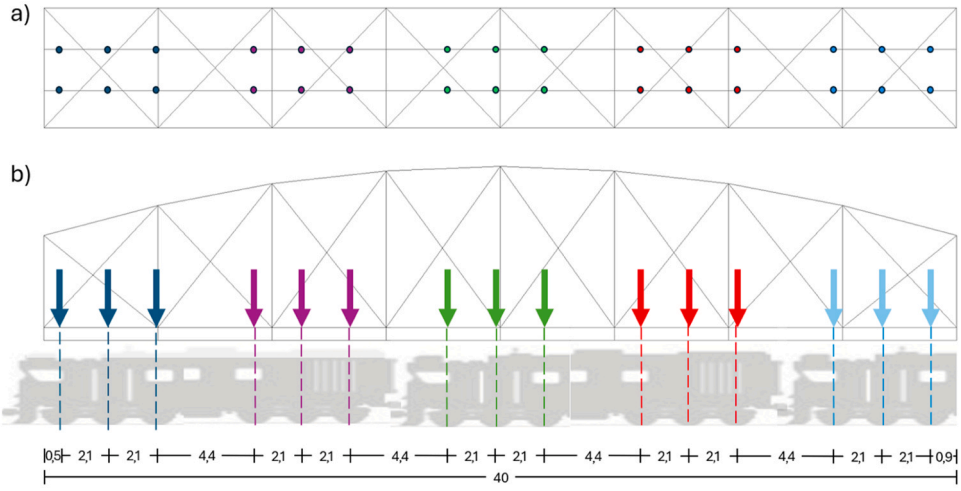

Fig. 5. Critical load position in the steel truss bridge, measurements in meters. (a) Plan view (b) Lateral view.

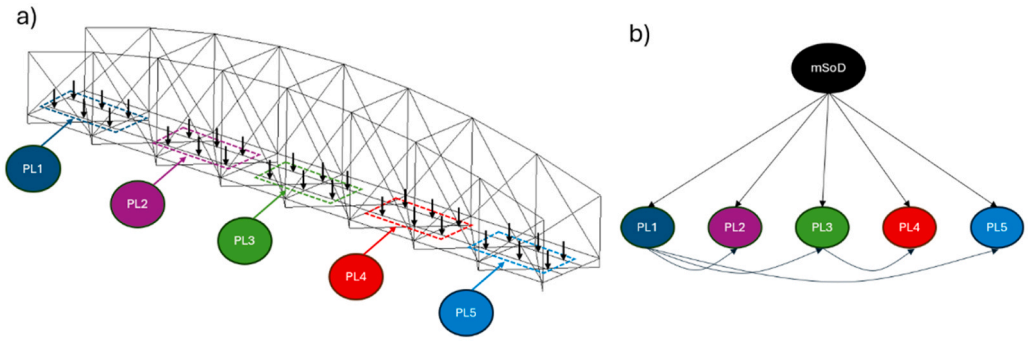

Fig. 6. Illustrating the creation of the GCBN. (a) Load nodes (b) Initial DAG.

distributions of the remaining nodes in the GCBN are determined based on the conditionalized value of one or more variables. In this study, the mSoD node was conditionalized to a value of 19 %, identified through the package-based analysis as the maximum mSoD observed across simulation groups. Fig. 9 illustrates the exceedance probability for the load nodes, both with and without conditioning in the mSoD node. These graphs show that conditionalizing the mSoD results in load distributions skewed towards higher values across all cases. This is particularly beneficial compared to conventional sampling methods that do not incorporate the effects of structural response to generate loading conditions for the bridge. For instance, a conventional approach might treat load variables as independent, failing to capture their interaction with the overall demand state.

3.2.2. *Selection of relevant member failures*

Relevant member failures were selected following a threat-independent approach [95]. Each member failure scenario was numerically generated in the UFEM without considering the specific hazard that led to the scenario (e.g. fatigue). The selection of relevant member failure scenarios was based on two complementary criteria: historical precedents of failure propagation in steel truss bridges and an in-service assessment of the studied structure. For the first criterion, a threat-independent approach was adopted, meaning that the simulated failures were not associated with specific hazards (e.g. fatigue), but rather focused on members whose failure triggered the progressive collapse of the entire structure or significant portions of it. This selection was supported by a previous study by the authors [96], which analysed 25 documented bridge collapses and identified the elements whose failure led to propagation across the structure. That study compiled detailed information on the initial damage, its propagation patterns, and associated consequences to each collapse, allowing for the identification of critical elements with a history of inducing severe structural effects. This increased the relevance and interest of the selected elements for the current case study. The second criterion was based on an in-service assessment of the bridge. To this end, the UFEM was used to compute the SoD for all structural elements under service conditions (undamaged), enabling the identification of elements with higher demands in comparison to their capacity. Together, these two strategies provided a consistent basis for selecting failure scenarios that are both historically grounded and structurally meaningful in the context of the studied bridge. Fig. 10 and Table 1 highlight the member failure scenarios considered. The numbers in the figure correspond to the identification IDs of each scenario.

The simulation approach follows the methodology outlined in Section 2, as depicted in the flowchart in Fig. 1. It was considered 10 heavy train crossings per day. Thus, 3650 loading samples were generated with the GCBN, representing a year of operational conditions. Each failure scenario was simulated in the UFEM, and the SoD was computed for all bridge elements. The resulting dataset, which consists of SoD values for all bridge elements when the bridge is subjected to all member failure scenarios (FS1 to FS11). The key modelling and computational parameters of the analysis are summarised in Table 2. This table outlines the core aspects of the methodology, including the UFEM configuration, uncertainty quantification, number of simulations, computational setup, and post-processing strategies (see Section 2). The information is presented to provide transparency on the computational cost and scope of the analysis, facilitating comparison with other approaches that assess member failure scenarios in steel truss bridges. The assessment of

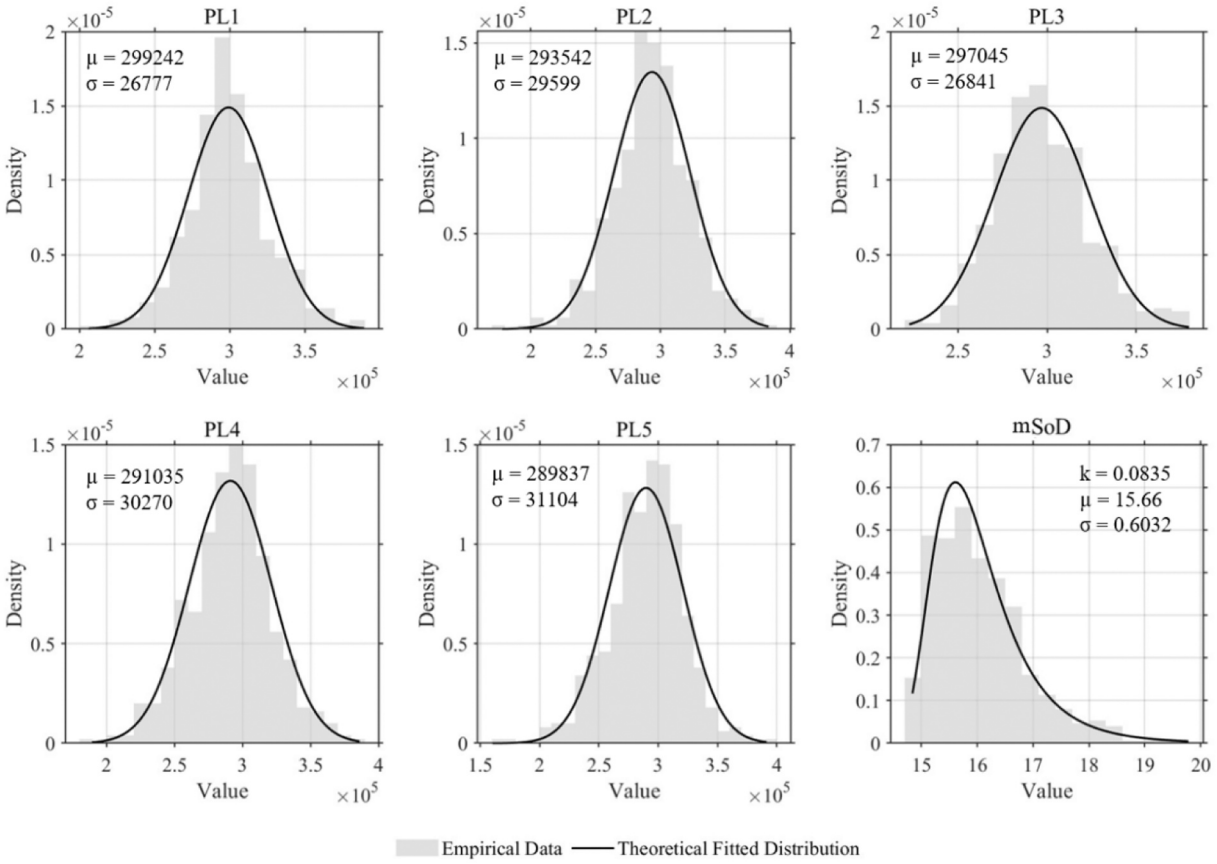

Fig. 7. Theoretical fitted distributions for the load nodes -PL1 to PL5- and the structural response (mSoD). Measurements of μ and σ in kN.

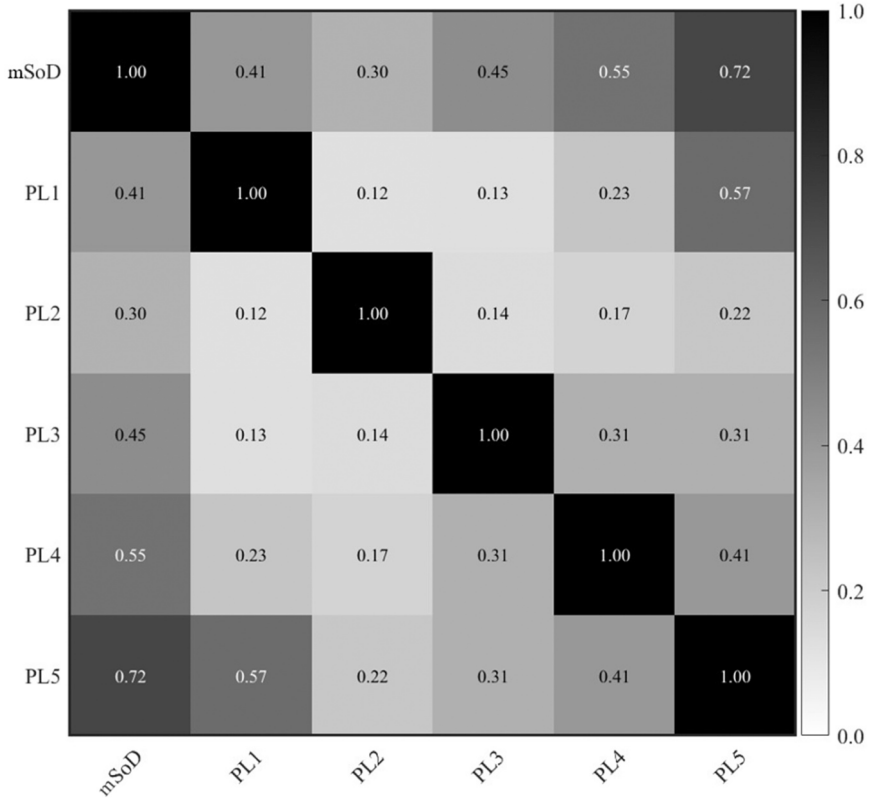

Fig. 8. Gaussian Copula-based Bayesian Network rank correlation matrix.

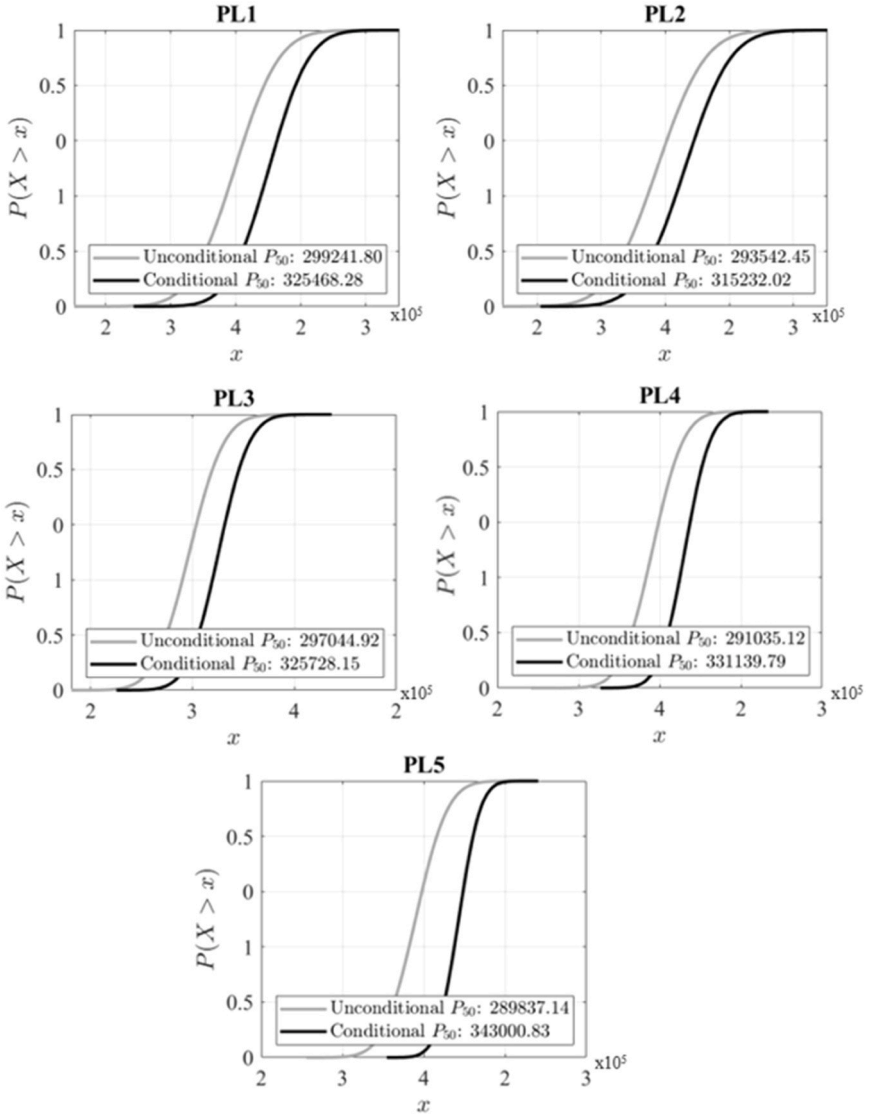

Fig. 9. Conditional margin for all nodes (PL1 to PL5) in the GCBN.

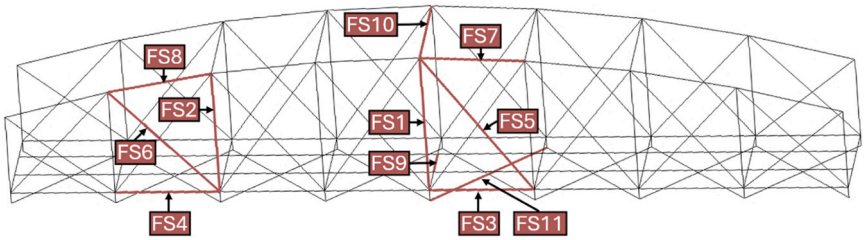

Fig. 10. Member failure scenarios considered.

member failure scenarios is discussed in the following section.

3.3. Assessment of member failure scenarios

Understanding the structural implications of localised member failures is essential for assessing the behaviour of steel truss bridges. This section shows how the methodology presented in Section 2.4 applies to the case study. Starting with the derivation of the $SoDT_{100}$ metric and building upon the described in Section 2.4. The analysis is carried out using two complementary approaches. The structure-level analysis examines how specific failure events impact the bridge elements, offering insight into the level of significance of the scenarios. In contrast, the element-based analysis focuses on the response of specific bridge elements when the bridge is subjected for all member failure scenarios, allowing for the identification of groups of elements that should be prioritized in SHM system and maintenance interventions. Together, these approaches comprehensively evaluate member failures and their effects on the bridge.

Table 1
List of member failure scenarios.

Scenario ID	Failure Scenario
FS1	Vertical No. 7
FS2	Vertical No. 3
FS3	Lower Chord No. 11
FS4	Lower Chord No. 3
FS5	Diagonal No. 33
FS6	Diagonal No. 9
FS7	Upper Chord No. 9
FS8	Upper Chord No. 3
FS9	Transversal Beam No. 14
FS10	Upper Transversal Beam No. 3
FS11	Lateral Bracing No. 10

Table 2
Key modelling and computational parameters for the case study.

Parameter	Value / Description
Model type	Updated Finite Element Model (UFEM).
Uncertainty modelled	Traffic loads (via GCBN).
Failure scenarios analysed	Eleven (11) member failure scenarios (threat-independent).
Load samples per scenario	3650 samples (1 year; 10 trains/day).
Total simulations	40,150 UFEM analyses (11 × 3650).
Simulation type	Nonlinear static for each load sample.
Index	State of Demand
Index calculation	Computed for each bridge element.
CPU cores used	16 (Intel Xeon)
Average time per scenario	~30 h
Post-processing	Statistical fitting of SoD indexes; Extreme Value Analysis to compute SoD_{T100}
Main outputs	Matrix of SoD_{T100} [Elements × Scenarios]
Final insights	Element-based insights to optimise SHM strategies, prioritise maintenance interventions, and enhancing reliability-based and risk methodologies.

3.3.1. The 100-year return period expected value of the SoD

The assessment of member failure scenarios considers estimating the 100-years return period expected value of SoD ($SoDT_{100}$) for all bridge elements. As described in 2.3, EVA is implemented to characterise the extreme structural responses. The daily maxima of the SoD were extracted for all bridge elements, providing a single critical value that represents the maximum demand observed per day. These daily maxima were then fitted to a Generalized Extreme Value (GEV) distribution using maximum Likelihood estimation (MLE) to calculate the expected SoD values for different return periods. This procedure was performed for all bridge elements when the bridge was undamaged and subjected to all member failure scenarios (FS1 to FS11). Thus, during each scenario, $SoDT_{100}$ is computed for all bridge elements. Fig. 11 exemplifies the process. The figure displays the probability of excedeence of the SoD of a midspan vertical of the bridge (Vertical 7) when: (a) The bridge is in its undamaged state, (b) the bridge is subjected to a close-to-support vertical failure (FS2), and (c) the bridge subjected to a midspan lower chord (FS3). In the figure, the blue points represent the observed daily maxima (from UFEM simulations), while the red points correspond to the estimated values derived from the GEV distribution. As discussed in section 2.3, the resulting $SoDT_{100}$ values establish a consistent basis to assess the significance of each failure scenario, forming the foundation for the analytical approaches introduced in the following sections.

3.3.2. Structure-level analysis

The structure-level analysis was performed as described in 2.4.1. This approach focusses in analysing how a specific member failure scenario (e.g. FS2) affects the $SoDT_{100}$ of all bridge elements (e.g. lower chords). The Eq. (2) was implemented to compute for all bridge elements the absolute increase of the $SoDT_{100}$ when the bridge is subjected to a failure scenario with its undamaged state (See 2.4). The results are displayed in Fig. 12.

Each truss representation in Fig. 12 corresponds to a specific failure event, where the removed element is marked, and the remaining elements are colour-coded based on the magnitude of their $\Delta SoDT_{100}$ as indicated in the colour-bar legend on the right side of the figure. Elements with low variations of $SoDT_{100}$ with respect to its undamaged state (0–5 %) remain grey, while those experiencing higher increases are classified as green (5–25 %), yellow (25–60 %), orange (60–100 %), and

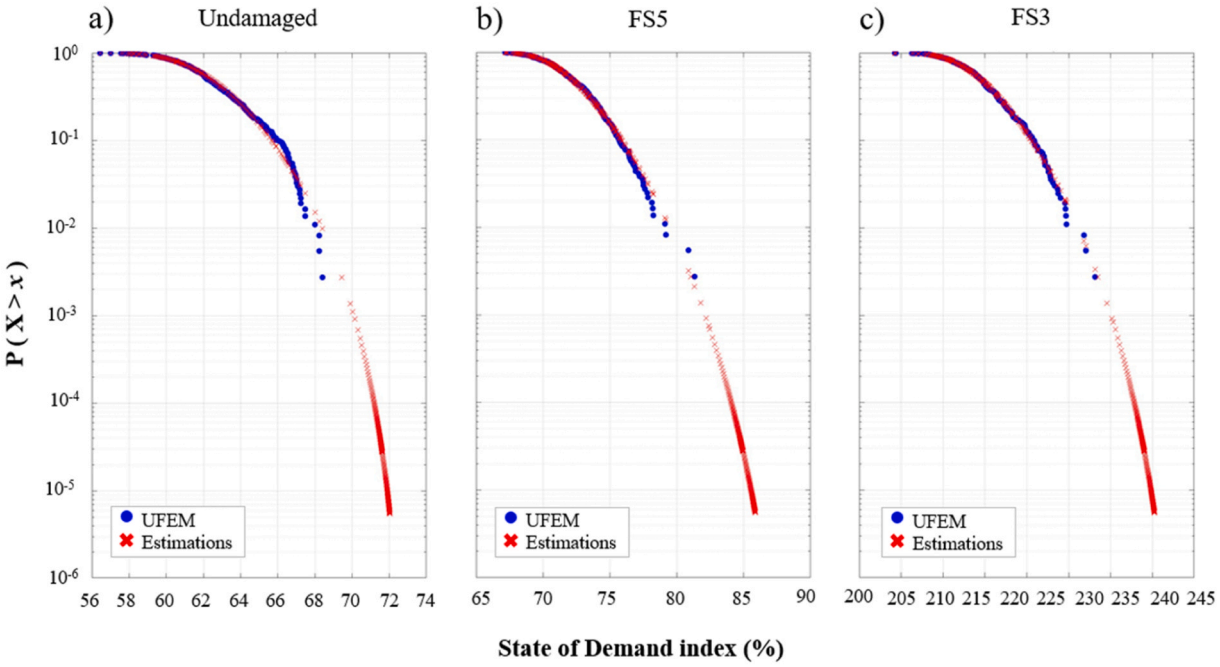

Fig. 11. EVA to estimate the SoD expected value for different return periods. Probability of exceedance of SoD for Vertical 7 (a) Undamaged state (b) FS2 (c) FS3.

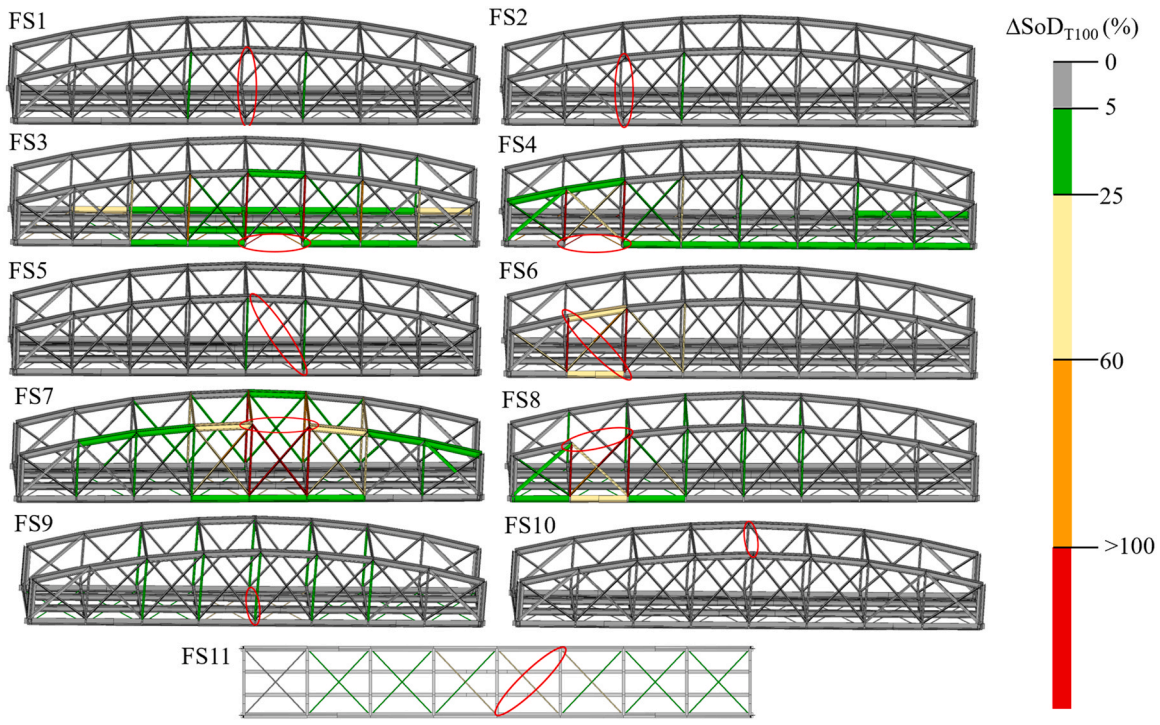

Fig. 12. $\Delta SoDT_{100}$ in all bridge elements for all member failure scenarios.

red (above 100 %). As observed in Fig. 12, failure scenarios that lead to significant increases in $\Delta SoDT_{100}$ across multiple bridge elements are those involving upper chords, lower chords, and diagonal members. More specifically, scenarios where central upper and lower chords fail (FS3 and FS7) and those where upper chords, lower chords, and diagonals near the supports fail (FS4, FS6 and FS8) exhibit the highest increases for the remaining bridge elements.

The failure of a central upper chord (FS7) produces the widest SoD distribution across the structure. The entire panel containing the failed element exhibits a severe increase, with both verticals and diagonals turning red. Additionally, adjacent panels also experience increments, with their diagonals turning yellow, indicating that the effects extend beyond the immediate vicinity of the failure. As described in Section 2.1, the SoD reflects variations in the structural demand-to-capacity ratio, allowing for an assessment of how failure scenarios alter the overall behaviour of the system. Based on these results, it can be inferred that upper chords in midspan play a fundamental role in transferring demand across multiple panels, as their removal leads to widespread SoD increases in surrounding elements. In contrast, when an upper chord near the support fails (FS8), the affected area is more localised. While the panel containing the failed element still exhibits high values, the effect on adjacent panels is less pronounced. This indicates that upper chords at midspan are more structurally engaged in global distribution, whereas those near the supports experience more localised effects. On another hand, a distinct pattern is observed for lower chords. When a midspan lower chord fails (FS3), the adjacent verticals exhibit high SoD values, but unlike the upper chord failure, the entire panel does not experience a uniform increase since there are more elements providing capacity in the bottom part of the bridge (e.g. bracing). Additionally, FS3 shows that internal longitudinal beams exhibit an increase in SoD, which is not observed in upper chord failures, suggesting that lower chords influence the internal bracing system more directly. When a lower chord near the support fails (FS4), the behaviour is comparable to FS3 but with one notable difference: multiple lower chords in the longitudinal direction exhibit slight increases. This suggests that lower chords near the support contribute more significantly to longitudinal demand transmission than those at midspan. The failure of a diagonal near the support (FS7) produces a markedly different response compared to midspan diagonal failures. While the failure of a central diagonal (FS5) induces only minor $\Delta SoDT_{100}$ increases in adjacent verticals, the removal of a diagonal near the support results in severe increases in surrounding verticals, reaching the red threshold in Fig. 12.

Beyond these primary failure scenarios, other elements exhibit distinct SoD responses under localised failures. The failure of a vertical does not lead to significant increases in other elements, except on those adjacent to the failed, which experience a slight increase (FS1 and FS2). This suggests that verticals primarily act as local demand distributors, and their failure does not substantially impact the overall truss response. A unique pattern is observed in lateral bracing failures (FS11). Unlike other elements, when a lateral bracing member fails, SoD increases are distributed only across multiple bracings, including those farther from the failed element. This indicates that lateral bracings exhibit a demand-sharing effect, where failure in one member influences a broader region of the structure. Similarly, the failure of a transversal beam at midspan (FS9) results in a widespread but moderate SoD increase, primarily affecting lateral bracing members and verticals. While the magnitude of the SoD increase remains low (classified as green in Fig. 12), the broad effect suggests that transversal beams contribute to structural demand distribution across multiple elements. Finally, the failure of an upper transversal beam (FS10) does not result in any SoD increases in other bridge elements, indicating that these members play a negligible role in the redistribution of structural demand under the analysed and vertical loading conditions.

As outlined in Section 2.4.1, the member failure scenarios discussed above are classified based on their level of significance. This classification provides a structured understanding of how different localised failures affect the overall truss system. Table 3 presents the classification of each scenario.

3.3.3. *Element-based analysis*

The element-based analysis provides an alternative perspective for evaluating the impact of localised failures in truss bridges. Instead of analysing individual failure scenarios, this approach focuses on how different groups of elements respond to different failure events. As

Table 3
Scenario-based classification of different member failures.

Scenario ID	Failure Scenario	Level of significance
FS1	Vertical No. 7	Low
FS2	Vertical No. 3	Low
FS3	Lower Chord No. 11	Medium-high
FS4	Lower Chord No. 3	Medium-high
FS5	Diagonal No. 33	Low
FS6	Diagonal No. 9	High
FS7	Upper Chord No. 9	High
FS8	Upper Chord No. 3	Medium-high
FS9	Transversal Beam No. 14	Medium
FS10	Upper Transversal Beam No. 3	Non-significant
FS11	Lateral Bracing No. 10	Medium

described in Section 2.4.2, this method enables the identification of elements that play a critical role in alternative load path formation, as well as those that should be prioritised in structural health monitoring (SHM) and maintenance strategies. To systematically assess the structural response, Fig. 13 presents a graphical representation where the Y-axis corresponds to the $\Delta SoDT_{100}$, indicating the demand state of each element for a 100-year return period, while the X-axis groups the elements into structural categories. Each failure scenario is represented by a unique colour-coded point, corresponding to the $SoDT_{100}$ value of the affected elements when the bridge is subjected to that scenario. The colour legend in Fig. 13 indicates the failure scenario ID (FS1–FS11) associated with each data point, allowing direct comparison between scenarios. Additionally, a solid line is plotted across all structural groups, representing the undamaged state of each element category. Any point above this reference line indicates an increase in the $SoDT_{100}$ due to a failure scenario, highlighting the most affected elements. This visualization provides an intuitive understanding of the structural impact of different failure scenarios. By grouping elements, the approach facilitates the identification of structural categories that exhibit greater sensitivity to localised failures. This classification is particularly relevant for SHM and maintenance prioritisation, as it allows engineers to determine which bridge elements are more vulnerable under various failure conditions.

In Fig. 13, among all structural groups, verticals exhibit the highest sensitivity, consistently experiencing the most significant changes across multiple failure scenarios. While the removal of a vertical itself does not lead to major alterations in the surrounding elements, verticals are particularly affected by failures in upper chords (FS7, FS8), lower chords (FS3, FS4), and diagonals near supports (FS6). This reinforces the role of verticals as load distributors, which do not initiate major redistributions when failing but are highly responsive to failures in primary load-bearing components. A similar but less pronounced trend is observed in diagonals, which are particularly influenced by upper chord failures at midspan and near supports. This highlights the role of diagonals in stabilizing the truss system when chords are compromised but also suggests that diagonals themselves are less involved in large-scale redistributions when removed. Chords themselves exhibit contrasting behaviour. While chord failures have a significant impact on the rest of the truss, the chords are minimally affected by failures in other elements. This contrasts with verticals, which are highly influenced by failures in other members but do not cause major redistributions when failing. This distinction underscores the primary function of chords as direct load carriers, while verticals and diagonals serve as secondary stabilizing components that adapt to redistribution demands. Another key finding is the dependency of lateral bracings on lower chord failure scenarios. Unlike other elements, lateral bracings primarily respond to lower chord failures (FS3, FS4), with upper chord failures having minimal impact. This suggests that lateral bracings play a localised stabilizing role as well as elements that provide resistant capacity at the bottom part of the bridge. Finally, for upper transversal beams, the only notable effect is seen under midspan upper chord failures (FS7). This limited response indicates that these elements contribute to localised panel stability, but do not participate significantly in global redistribution mechanisms.

4. Conclusions

This study proposes a methodology for assessing the structural response of steel truss bridges subjected to localized member failures. The proposed approach integrates numerical modelling, structural performance metrics, and statistical tools to evaluate the consequences of member failures at both structure and element levels. A State-of-Demand index (SoD) is implemented as a quantitative metric to evaluate the relationship between demand and capacity when the bridge is subjected to failure scenarios. Additionally, a Gaussian Copula-based Bayesian Network (GCBN) is developed to model the probabilistic relationship between load conditions and structural response and Extreme Value Analysis (EVA) is applied to estimate the expected SoD for a 100-year return period.

The methodology was applied to an old-riveted steel truss bridge,

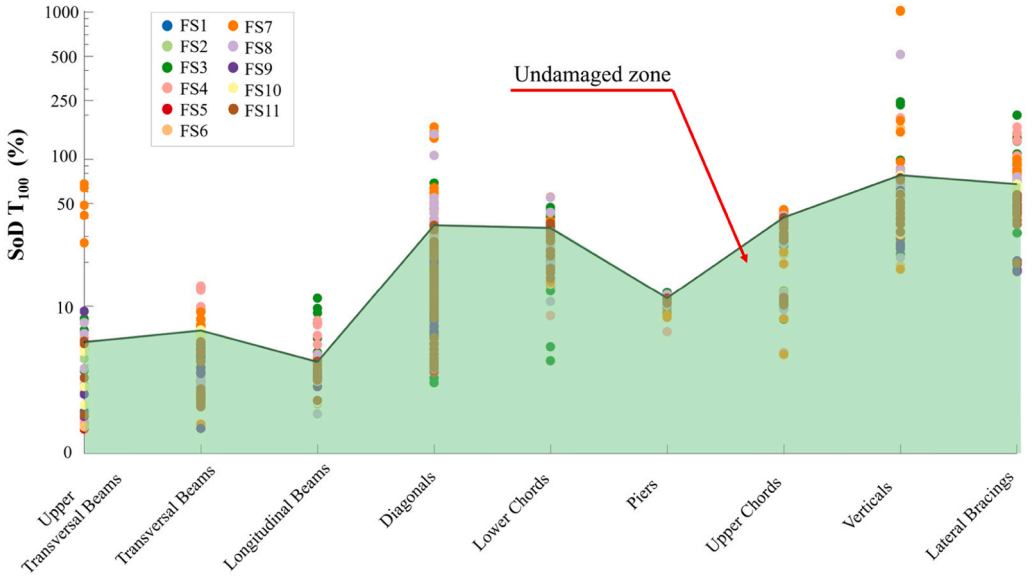

Fig. 13. Element-based analysis of member failure scenarios.

which was selected due to its historical significance and available monitoring data. Eleven member failure scenarios were considered based on documented precedents of progressive collapse in steel truss bridges and an in-service structural assessment. Each scenario was simulated using an Updated Finite Element Model (UFEM) to evaluate its consequences on the bridge elements. Of the eleven scenarios considered, the analysis identified failures involving upper and lower chords and diagonals near supports as the most significant, as they induced significant demand increases across multiple bridge elements. Specifically, upper chord failures caused the expected increase in $\Delta SoDT_{100}$ to exceed 100 % in nearly all elements adjacent to the failed member, while inducing demand increases between 60 % and 100 % in the rest of the structure. Failures in lower chords and diagonals near supports led to $\Delta SoDT_{100}$ surges above 100 % in verticals, while other elements experienced increases ranging from 25 % to 60 %. In contrast, strut failures primarily resulted in localized demand variations, with minimal influence on surrounding elements. The above findings suggest the need to prioritise upper and lower chords and diagonals near support, as its failure implies the triggering of significant demand redistributions across most of the truss system.

The proposed methodology bridges the gap between scientific research and practical engineering applications. By integrating finite element modelling, performance metrics and statistical analysis, it offers a systematic framework for evaluating the structural consequences of steel truss bridges subjected to localized failures. The methodology contributes to optimise SHM strategies, prioritise maintenance interventions, and enhancing reliability-based and risk methodologies. Ultimately, the findings of this research aim to support the decision of authorities regarding bridge safety, monitoring, and maintenance.

CRediT authorship contribution statement

Adam Jose: Writing – original draft, Supervision, Funding acquisition. **Oswaldo Morales-Nápoles:** Writing – review & editing, Investigation, Formal analysis. **Manuel Buitrago:** Writing – review & editing, Formal analysis. **Brais Barros:** Writing – review & editing, Investigation, Formal analysis. **Santiago López:** Writing – review & editing, Writing – original draft, Investigation, Formal analysis. **Belen Riveiro:** Writing – review & editing, Writing – original draft, Supervision, Funding acquisition.

Declaration of Competing Interest

The authors declare that they have no known competing financial interests or personal relationships that could have appeared to influence the work reported in this paper.Jose M. Adam and Belén Riveiro report financial support provided by the PONT3 project (ref: PID2021–124236OB).

Acknowledgements

The authors wish to acknowledge the grant awarded for the Pont3 project (ref: PID2021–124236OB) funded by MCIN/AEI/ 10.13039/ 50110001103.

Data availability

Data will be made available on request.

References

[1] Field CB, Barros V, Stocker TF, Dahe Q. Managing the Risks of Extreme Events and Disasters to Advance Climate Change Adaptation: Special Report of the Intergovernmental Panel on Climate Change. Cambridge University Press; 2012.
[2] Adam JM, Makoond N, Riveiro B, Buitrago M. “Risks of bridge collapses are real and set to rise — here’s why,”. Nature 2024;629(8014):1001–3. https://doi.org/10.1038/d41586-024-01522-6.
[3] Serdar MZ, Koç M, Al-Ghamdi SG. “Urban transportation networks resilience: indicators, disturbances, and assessment methods,”. Sustain Cities Soc Jan. 2022; 76:103452. https://doi.org/10.1016/j.scs.2021.103452.
[4] Starossek U. Progressive collapse of structures. Thomas Telford Lond 2009;153.
[5] Adam JM, Parisi F, Sagaseta J, Lu X. “Research and practice on progressive collapse and robustness of building structures in the 21st century,”. Eng Struct 2018;173: 122–49. https://doi.org/10.1016/j.engstruct.2018.06.082.
[6] Kiakojouri F, De Biagi V, Marchelli M, Chiaia B. “A conceptual note on the definition of initial failure in progressive collapse scenarios,”. Structures 2024;60: 105921. https://doi.org/10.1016/j.istruc.2024.105921.
[7] Choudhury JR, Hasnat A. “Bridge collapses around the world: causes and mechanisms,”. IABSEJSCE Jt Conf Adv Bridge EngIII Dhaka Bangladesh 2015: 26–34.
[8] Deng L, Wang W, Yu Y. “State-of-the-art review on the causes and mechanisms of bridge collapse,”. J Perform Constr Facil 2016;30(2). https://doi.org/10.1061/(ASCE)CF.1943-5509.0000731.
[9] Dexter RJ, Connor RJ, Mahmoud H. “Review of steel bridges with fracture-critical elements,”. Transp Res Rec J Transp Res Board 2005;1928(1):74–82. https://doi.org/10.1177/0361198105192800108.
[10] Gerasimidis S, Ellingwood B. “Twenty years of advances in disproportionate collapse research and best practices since 9/11/2001,”. J Struct Eng 2023;149(2). https://doi.org/10.1061/JSENDH.STENG-12056.
[11] Derseh SA, Mohammed TA. “Bridge structures under progressive collapse: a comprehensive state-of-the-art review,”. Results Eng 2023;18:101090. https://doi.org/10.1016/j.rineng.2023.101090.
[12] Elkady N, Augusthus Nelson L, Weekes L, Makoond N, Buitrago M. “Progressive collapse: Past, present, future and beyond,”. Structures 2024;62:106131. https://doi.org/10.1016/j.istruc.2024.106131.
[13] Buitrago M, Bertolesi E, Calderón PA, Adam JM. “Robustness of steel truss bridges: Laboratory testing of a full-scale 21-metre bridge span,”. Structures 2021;29: 691–700. https://doi.org/10.1016/j.istruc.2020.12.005.
[14] Brunell G, Kim YJ. “Effect of local damage on the behavior of a laboratory-scale steel truss bridge,”. Eng Struct 2013;48:281–91. https://doi.org/10.1016/j.engstruct.2012.09.017.
[15] Zhao X, Yan S, Chen Y, Xu Z, Lu Y. “Experimental study on progressive collapse-resistant behavior of planar trusses,”. Eng Struct 2017;135:104–16. https://doi.org/10.1016/j.engstruct.2016.12.013.
[16] Porcu MC, Buitrago M, Calderón PA, Garau M, Cocco MF, Adam JM. “Robustness-based assessment and monitoring of steel truss railway bridges to prevent progressive collapse,”. J Constr Steel Res 2025;226:109200. https://doi.org/10.1016/j.jcsr.2024.109200.
[17] Caredda G, Porcu MC, Buitrago M, Bertolesi E, Adam JM. “Analysing local failure scenarios to assess the robustness of steel truss-type bridges,”. Eng Struct 2022;262. https://doi.org/10.1016/j.engstruct.2022.114341.
[18] Chen X, Li H, Agrawal AK, Ettouney M, Wang H. “Alternate load paths redundancy analysis of steel truss bridges,”. J Bridge Eng 2022;27(11). https://doi.org/10.1061/(ASCE)BE.1943-5592.0001943.
[19] Praxedes C, Yuan X-X, He X-H-C. “A novel robustness index for progressive collapse analysis of structures considering the full risk spectrum of damage evolution,”. Struct Infrastruct Eng 2022;18(3):376–94. https://doi.org/10.1080/15732479.2020.1851730.
[20] Li H, Agrawal AK, Chen X, Ettouney M, Wang H. “A framework for identification of the critical members for truss bridges through nonlinear dynamic analysis,”. J Bridge Eng 2022;27(8). https://doi.org/10.1061/(ASCE)BE.1943-5592.0001902.
[21] Connor RJ, Martín FJB, Varma A, Lai Z, Korkmaz C. Fracture-Critical System Analysis for Steel Bridges. Washington, D.C.: Transportation Research Board; 2018. https://doi.org/10.17226/25230.
[22] Liu S, Bartlett FM, Zhou W. “Alternative load paths in steel through-truss bridges: case study,”. J Bridge Eng 2013;18(9):920–8. https://doi.org/10.1061/(ASCE)BE.1943-5592.0000436.
[23] Lin W, et al. After-fracture redundancy analysis of an aged truss bridge in Japan. Struct Infrastruct Eng 2017;13(1):107–17. https://doi.org/10.1080/15732479.2016.1198393.
[24] Yamaguchi E, Okamoto R, Yamada K. “Post-member-failure analysis method of steel truss bridge,”. Procedia Eng 2011;14:656–61. https://doi.org/10.1016/j.proeng.2011.07.083.
[25] Chen X, Li H, Agrawal AK, Ettouney M, Wang H. “Performance-based retrofits of long-span truss bridges based on the alternate load path redundancy analysis,”. J Bridge Eng 2023;28(2). https://doi.org/10.1061/JBENF2.BEENG-5354.
[26] Li H, Shen L, Deng S. “A generalized framework for the alternate load path redundancy analysis of steel truss bridges subjected to sudden member loss scenarios,”. Buildings 2022;12(10):1597. https://doi.org/10.3390/buildings12101597.
[27] AASHTO. “Guide specifications for analysis and identification of fracture critical members and system redundant members,”. AASHTO Wash Dc [Online] 2022. ⟨https://store.transportation.org/Item/PublicationDetail?ID=4141⟩ (Available).
[28] AASHTO, “Guide specifications for internal redundancy of mechanically-fastened built-up steel members,” AASHTO Washington, DC, Washington, 2018. Accessed: Nov. 05, 2024. [Online]. Available: ⟨https://store.transportation.org/Item/PublicationDetail?ID=4149&AspxAutoDetectCookieSupport=1⟩.
[29] Baker JW, Schubert M, Faber MH. “On the assessment of robustness,”. Struct Saf 2008;30(3):253–67. https://doi.org/10.1016/j.strusafe.2006.11.004.
[30] Hendawi S, Frangopol DM. “System reliability and redundancy in structural design and evaluation,”. Struct Saf 1994;16(1–2):47–71. https://doi.org/10.1016/0167-4730(94)00027-N.

[31] Casas JR, Frangopol DM, Turmo J, Tsompanakis Y. "Bridge safety assessment, maintenance, monitoring, and life-cycle performance,". Struct Infrastruct Eng 2024;20(7–8):957–9. https://doi.org/10.1080/15732479.2024.2331082.

[32] Hammervold J, Reenaas M, Brattebø H. "Environmental life cycle assessment of bridges,". J Bridge Eng 2013;18(2):153–61. https://doi.org/10.1061/(ASCE)BE.1943-5592.0000328.

[33] Frangopol DM, Strauss A, Kim S. "Bridge reliability assessment based on monitoring,". J Bridge Eng 2008;13(3):258–70. https://doi.org/10.1061/(ASCE)1084-0702(2008)13:3(258).

[34] Kiureghian ADer. "Analysis of structural reliability under parameter uncertainties,". Probabilistic Eng Mech 2008;23(4):351–8. https://doi.org/10.1016/j.probengmech.2007.10.011.

[35] Nassar M, Guizani L, Nollet M-J, Tahan A. "Effects of temperature, analysis and modelling uncertainties on the reliability of base-isolated bridges in Eastern Canada,". Structures 2022;37:295–304. https://doi.org/10.1016/j.istruc.2022.01.023.

[36] Nassar M, Guizani L, Nollet M-J, Tahan A. "A probability-based reliability assessment approach of seismic base-isolated bridges in cold regions,". Eng Struct 2019;197:109353. https://doi.org/10.1016/j.engstruct.2019.109353.

[37] Hohenbichler M, Gollwitzer S, Kruse W, Rackwitz R. "New light on first- and second-order reliability methods,". Struct Saf 1987;4(4):267–84. https://doi.org/10.1016/0167-4730(87)90002-6.

[38] Rajashekhar MR, Ellingwood BR. "A new look at the response surface approach for reliability analysis,". Struct Saf 1993;12(3):205–20. https://doi.org/10.1016/0167-4730(93)90003-J.

[39] Tabandeh A, Jia G, Gardoni P. "A review and assessment of importance sampling methods for reliability analysis,". Struct Saf 2022;97:102216. https://doi.org/10.1016/j.strusafe.2022.102216.

[40] Langseth H, Portinale L. "Bayesian networks in reliability,". Reliab Eng Syst Saf 2007;92(1):92–108. https://doi.org/10.1016/j.ress.2005.11.037.

[41] Portinale L, Bobbio A. "Bayesian networks for dependability analysis: an application to digital control reliability,". arXiv Prepr arXiv 2013;1301:*6734*.

[42] Torres-Toledano JG, Sucar LE. "Bayesian networks for reliability analysis of complex systems,". Prog Artif IntellIBERAMIA 98 6th IberoAm Conf AI Lisbon Port Oct 59 1998 Proc 1998;6:195–206.

[43] Cai B, et al. Application of Bayesian Networks in Reliability Evaluation. IEEE Trans Ind Inf 2019;15(4):2146–57. https://doi.org/10.1109/TII.2018.2858281.

[44] Tan J, Fang S. "Safety evaluation of truss bridges using continuous Bayesian networks,". Struct Control Health Monit 2022;29(4). https://doi.org/10.1002/stc.2912.

[45] Luque J, Straub D. "Reliability analysis and updating of deteriorating systems with dynamic Bayesian networks,". Struct Saf 2016;62:34–46. https://doi.org/10.1016/j.strusafe.2016.03.004.

[46] Maroni A, Tubaldi E, Val DV, McDonald H, Zonta D. "Using Bayesian networks for the assessment of underwater scour for road and railway bridges,". Struct Health Monit 2021;20(5):2446–60. https://doi.org/10.1177/1475921720956579.

[47] Gehl P, D'Ayala D. "Development of Bayesian Networks for the multi-hazard fragility assessment of bridge systems,". Struct Saf 2016;60:37–46. https://doi.org/10.1016/j.strusafe.2016.01.006.

[48] Salamatian SA, Zarrati AR, Banazadeh M. "Assessment of bridge safety due to scour by Bayesian network,". Proc Inst Civ Eng Water Manag 2013;166(6):341–50. https://doi.org/10.1680/wama.11.00071.

[49] Mendoza-Lugo MA, Delgado-Hernández DJ, Morales-Nápoles O. "Reliability analysis of reinforced concrete vehicle bridges columns using non-parametric Bayesian networks,". Eng Struct 2019;188:178–87. https://doi.org/10.1016/j.engstruct.2019.03.011.

[50] Tubaldi E, Turchetti F, Ozer E, Fayaz J, Gehl P, Galasso C. "A Bayesian network-based probabilistic framework for updating aftershock risk of bridges,". Earthq Eng Struct Dyn 2022;51(10):2496–519. https://doi.org/10.1002/eqe.3698.

[51] Luque J, Straub D. "Risk-based optimal inspection strategies for structural systems using dynamic Bayesian networks,". Struct Saf 2019;76:68–80. https://doi.org/10.1016/j.strusafe.2018.08.002.

[52] Chen T-T, Wang C-H. "Fall risk assessment of bridge construction using Bayesian network transferring from fault tree analysis,". J Civ Eng Manag 2015;23(2):273–82. https://doi.org/10.3846/13923730.2015.1068841.

[53] Chen T-T, Leu S-S. "Fall risk assessment of cantilever bridge projects using Bayesian network,". Saf Sci 2014;70:161–71. https://doi.org/10.1016/j.ssci.2014.05.011.

[54] Sun X, Xin Y, Wang Z, Yuan M, Chen H. "Damage detection of steel truss bridges based on Gaussian Bayesian networks,". Buildings 2022;12(9):1463. https://doi.org/10.3390/buildings12091463.

[55] Prajapat K, Ray-Chaudhuri S. "Damage detection in railway truss bridges employing data sensitivity under Bayesian framework: a numerical investigation,". Shock Vib 2017;2017:1–9. https://doi.org/10.1155/2017/6423039.

[56] Yin T, Zhu H. "Probabilistic damage detection of a steel truss bridge model by optimally designed Bayesian neural network,". Sensors 2018;18(10):3371. https://doi.org/10.3390/s18103371.

[57] Arangio S, Beck JL. "Bayesian neural networks for bridge integrity assessment,". Struct Control Health Monit 2012;19(1):3–21. https://doi.org/10.1002/stc.420.

[58] Barros B, Conde B, Riveiro B, Morales-Nápoles O. "Gaussian Copula-based Bayesian network approach for characterizing spatial variability in aging steel bridges,". Struct Saf 2024;106:102403. https://doi.org/10.1016/j.strusafe.2023.102403.

[59] Keo SA, De Larrard T, Duprat F, Geoffroy S. "Enhancement of predictive bayesian network model for corrosion alarm of steel reinforcement with uncertainty of NDT measurements,". J Nondestr Eval 2023;42(2):51. https://doi.org/10.1007/s10921-023-00959-5.

[60] Rocchetta R, Broggi M, Huchet Q, Patelli E. "On-line Bayesian model updating for structural health monitoring,". Mech Syst Signal Process 2018;103:174–95. https://doi.org/10.1016/j.ymssp.2017.10.015.

[61] Barros B, Conde B, Cabaleiro M, Riveiro B. "Deterministic and probabilistic-based model updating of aging steel bridges,". Structures 2023;54:89–105. https://doi.org/10.1016/j.istruc.2023.05.020.

[62] Morales-Nápoles O, Steenbergen RDJM. "Large-scale hybrid Bayesian network for traffic load modeling from weigh-in-motion system data,". J Bridge Eng 2015;20(1). https://doi.org/10.1061/(ASCE)BE.1943-5592.0000636.

[63] Mendoza-Lugo MA, Nogal M, Morales-Nápoles O. "Estimating bridge criticality due to extreme traffic loads in highway networks,". Eng Struct 2024;300:117172. https://doi.org/10.1016/j.engstruct.2023.117172.

[64] Kim J, Song J. "Bayesian updating methodology for probabilistic model of bridge traffic loads using in-service data of traffic environment,". Struct Infrastruct Eng 2023;19(1):77–92. https://doi.org/10.1080/15732479.2021.1924797.

[65] Yu Y, Cai CS, He W, Peng H. "Prediction of bridge maximum load effects under growing traffic using non-stationary bayesian method,". Eng Struct 2019;185:171–83. https://doi.org/10.1016/j.engstruct.2019.01.085.

[66] Gao X, Duan G, Lan C. "Bayesian updates for an extreme value distribution model of bridge traffic load effect based on SHM data,". Sustainability 2021;13(15):8631. https://doi.org/10.3390/su13158631.

[67] Morales-Nápoles O, Steenbergen RDJM. "Analysis of axle and vehicle load properties through Bayesian Networks based on Weigh-in-Motion data,". Reliab Eng Syst Saf 2014;125:153–64. https://doi.org/10.1016/j.ress.2014.01.018.

[68] Hanea A, Morales Napoles O, Ababei D. "Non-parametric Bayesian networks: Improving theory and reviewing applications,". Reliab Eng Syst Saf 2015;144:265–84. https://doi.org/10.1016/j.ress.2015.07.027.

[69] Cornell CA. "Bounds on the reliability of structural systems,". J Struct Div 1967;93(1):171–200. https://doi.org/10.1061/JSDEAG.0001577.

[70] OBrien EJ, et al. A review of probabilistic methods of assessment of load effects in bridges. Struct Saf 2015;53:44–56. https://doi.org/10.1016/j.strusafe.2015.01.002.

[71] E.J. Gumbel, "Statistics of Extremes," 1958, *Columbia University Press*.

[72] Nowak M, Straub D, Fischer O. "Statistical extrapolation for extreme traffic load effect estimation on bridges,". 14th International Probabilistic Workshop. Cham: Springer International Publishing; 2017. p. 135–53. https://doi.org/10.1007/978-3-319-47886-9_10.

[73] Embrechts P. "Extreme value theory: Potential and limitations as an integrated risk management tool,". Deriv Use Trading Regul 2000;6(1):449–56.

[74] Leadbetter MR. "On a basis for 'Peaks over Threshold' modeling,". Stat Probab Lett 1991;12(4):357–62.

[75] A. Ferreira and L.De Haan, "On the block maxima method in extreme value theory: PWM estimators," 2015.

[76] Kang S, Song J. "Parameter and quantile estimation for the generalized Pareto distribution in peaks over threshold framework,". J Korean Stat Soc 2017;46(4):487–501. https://doi.org/10.1016/j.jkss.2017.02.003.

[77] Box GEP, Cox DR. "An analysis of transformations,". J R Stat Soc Ser B Stat Method 1964;26(2):211–43.

[78] Rice SO. "Mathematical analysis of random noise,". Bell Syst Tech J 1944;23(3):282–332.

[79] Wang X, Ruan X, Casas JR, Zhang M. "Probabilistic model of traffic scenarios for extreme load effects in long-span bridges,". Struct Saf 2024;106:102382. https://doi.org/10.1016/j.strusafe.2023.102382.

[80] Wang X, Ruan X, Casas JR, Zhang M. "Probabilistic modeling of congested traffic scenarios on long-span bridges,". Appl Sci 2024;14(20):9525. https://doi.org/10.3390/app14209525.

[81] Rahman J, Aghaeidoost V, Billah AM. "Resilience of coastal bridges under extreme wave-induced loads,". Resilient Cities Struct 2024;3(2):85–100. https://doi.org/10.1016/j.rcns.2024.07.002.

[82] Dai B, Wu D, Li Q. "Investigation of multiple-presence factor for traffic loads on road-rail bridges based on a novel extreme value analysis approach,". Struct Saf 2022;96:102199. https://doi.org/10.1016/j.strusafe.2022.102199.

[83] European Committee for Standardization, "Eurocode 1: Actions on Structures. Part 2: Traffic Loads on Bridges - 2019," 2019.

[84] Wisniewski D, Casas JR, Ghosn M. "Load capacity evaluation of existing railway bridges based on robustness quantification,". Struct Eng Int 2006;16(2):161–6. https://doi.org/10.2749/101686606777962440.

[85] Zambrano A. "Determination of the critical loading conditions for bridges under crossing trains,". Eng Struct 2011;33(2):320–9. https://doi.org/10.1016/j.engstruct.2010.10.012.

[86] Mendoza-Lugo MA, Morales-Nápoles O. "Mapping hazardous locations on a road network due to extreme gross vehicle weights,". Reliab Eng Syst Saf 2024;242:109698. https://doi.org/10.1016/j.ress.2023.109698.

[87] Gomes MI, Guillou A. "Extreme value theory and statistics of univariate extremes: a review,". Int Stat Rev 2015;83(2):263–92. https://doi.org/10.1111/insr.12058.

[88] Salvadori G, De Michele C, Durante F. "On the return period and design in a multivariate framework,". Hydrol Earth Syst Sci 2011;15(11):3293–305. https://doi.org/10.5194/hess-15-3293-2011.

[89] Buxa, "River Eume's Railway Bridge," Asociacion Gallega de Patrimonio Industrial.

[90] European Committee for Standardization, "Eurocode 3: Design of steel structures. Part 2: Steel bridges," 1993.

[91] Paprotny D, Morales-Nápoles O, Worm DTH, Ragno E. "BANSHEE–A MATLAB toolbox for Non-Parametric Bayesian Networks,". SoftwareX 2020;12:100588. https://doi.org/10.1016/j.softx.2020.100588.

[92] Koot P, Mendoza-Lugo MA, Paprotny D, Morales-Nápoles O, Ragno E, Worm DTH. "PyBanshee version (1.0): A Python implementation of the MATLAB toolbox

BANSHEE for Non-Parametric Bayesian Networks with updated features,". SoftwareX 2023;21:101279. https://doi.org/10.1016/j.softx.2022.101279.
[93] Mendoza-Lugo MA, Morales-Nápoles O. "Version 1.3-BANSHEE—A MATLAB toolbox for Non-Parametric Bayesian Networks,". SoftwareX 2023;23:101479. https://doi.org/10.1016/j.softx.2023.101479.
[94] Dempster AP. "A Generalization of Bayesian Inference,". J R Stat Soc Ser B Stat Method 1968;30(2):205–32. https://doi.org/10.1111/j.2517-6161.1968.tb00722.x.
[95] Haberland M, Starossek U. "Progressive collapse nomenclature,". Structures Congress 2009. Reston, VA: American Society of Civil Engineers; 2009. p. 1–10. https://doi.org/10.1061/41031(341)209.
[96] López S, Makoond N, Sánchez-Rodríguez A, Adam JM, Riveiro B. "Learning from failure propagation in steel truss bridges,". Eng Fail Anal 2023;152. https://doi.org/10.1016/j.engfailanal.2023.107488.